Non-linear elastic moduli of Graphene sheet-reinforced polymer composites

Ahmed Elmarakbi[a], Wang Jianhua[b], Wiyao Leleng Azoti[a,*]

[a]*Faculty of Applied Sciences, University of Sunderland, Sunderland, UK, SR6 0DD*
[b]*College of Automotive Engineering, Jilin University, ChangChun, China, 130012*

Abstract

The non-linear elastic moduli of the Graphene sheet-reinforced polymer composite are investigated using a combined molecular mechanics theory and continuum homogenisation tools. Under uniaxial loading, the linear and non-linear constitutive equations of the Graphene sheet are derived from a Taylor series expansion in powers of strains. Based on the modified Morse potential, the elastic moduli and Poisson's ratio are obtained for the Graphene sheet leading to the derivation of the non-linear stiffness tensor. For homogenisation purpose, the strain concentration tensor is computed by the means of the irreducible decomposition of the Eshelby's tensor for an arbitrary domain. Therefore, a mathematical expression of the averaged Eshelby's tensor for a rectangular shape is obtained for the Graphene sheet. Under the Mori-Tanaka micro-mechanics scheme, the effective non-linear behaviour is predicted for various micro-parameters such as the aspect ratio and mass fractions. Numerical results highlight the effect of such micro-parameters on the anisotropic degree of the composite.

Keywords: Non-linear elastic moduli, Graphene sheet, Polymer composite, Eshelby's tensor, Mori-Tanaka scheme.

*Corresponding author. Tel. +44 (0)191 515 2684
Email address: `Wiyao.Azoti@sunderland.ac.uk` (Wiyao Leleng Azoti)

Nomenclature

α_1, α_2 Angle of the carbon bonds

$\Delta\alpha_1$, $\Delta\alpha_2$ Angle variations of the bonds

$\Delta\theta$ Angle variation for three neighbouring atoms

Δr Variation of bonding length

ϵ Applied strain

η Aspect ratio

ν Poisson's ratio

$\rho_{c,g,m}$ Density of the composite, Graphene, matrix

σ Observed stress

σ_x,σ_y Axial stress

τ_{xy} Shear stress

$\mathbf{A}_g$ Localisation tensor

$\mathbf{I}$ Identity tensor

$\mathbf{L}_g$ Linear stiffness tensor

$\mathbf{L}$ Effective linear stiffness tensor

$\mathbf{N}_g$ Non-linear stiffness tensor

$\mathbf{N}$ Effective non-linear stiffness tensor

$\mathbf{S}_0$ Isotropic part of the Eshelby's tensor

$\mathbf{S}_\omega$ Anisotropic part of the Eshelby's tensor

θ_i Interior points angles

D_g Non-linear modulus of the Graphene sheet

E_g Linear modulus of the Graphene sheet

i_1, i_2 Orthonormal basis vectors

M_g Mass fraction of the Graphene sheet

M_m Mass fraction of the matrix

p_2, q_2, p_4, q_4 Complex-variables of boundary integrals

r Bond length

t Thickness of the Graphene sheet

$U_{in-plane}$ Modified Morse potential

V_g Volume fraction of the Graphene sheet

V_m Volume fraction of the matrix

x, y Position vectors

z Relative position vectors

$\mathbf{i}$ Unit imaginary number

1. Introduction

Thanks to its remarkable physical and mechanical properties, Graphene has attracted extensive research investigations since its discovery in 2004 as reported by Cao (2014). Graphene is usually studied as two-dimensional structure because of its nano-scale thickness. For understanding the mechanical properties of Graphene, several attempts have been employed among which experimental measurements and theoretical developments as well as numerical modelling. The firsts i.e experiments provide the most effective way to measure the elastic modulus of Graphene. Different values of Young modulus are presented in the open literature. These values are essentially derived from the free standing indentation based on the Atomic Force Microscope (AFM). Works by Lee et al. (2008) and Frank et al. (2007) as well as Zhang and Pan (2012) should be cited. Moreover, much high elastic modulus has been estimated by Lee et al. (2012). Indeed, using a Raman Spectroscopy method they find values of 2.4 TPa and 2.0 TPa for a mono-layer and bilayer Graphene respectively. However, Cao (2014) highlights that the value of the Poisson's ratio cannot be directly measured by experiments. Therefore, theoretical and numerical studies have been developed based on the atomistic simulation at nano-scale and continuum/structural mechanics modelling. These studies deal essentially with quantum mechanics (QM) calculations for instance in Wei et al. (2009) and semi-empirical methods like thigh-biding used in Zhao et al. (2009); Cadelano et al. (2009) as well as molecular dynamics (MD) with empirical inter-atomic potentials studied by Zhao et al. (2009); Zhang et al. (2012); Wang and Zhang (2012); Lu et al. (2011); Sakhaee-Pour (2009); Zhou et al. (2013b,a); Sakhaee-Pour et al. (2008); Sakhaee-Pour (2009); Wang (2010); Lu and Huang (2009). Under large deformations, the elastic behaviour of the Graphene sheet must be considered non-linear. This implies the existence of an energy potential that is function of the strain which can be expressed as a Taylor series in powers of strain as presented by Lee et al. (2008). Therefore, the stress-strain relationship is described by two parameters: the linear elastic modulus E and the non-linear elastic modulus D. This relationship has been used by Cadelano et al. (2009) to derive the constitutive law and all non-linear moduli for the Graphene stretching elasticity. Works by Wei et al. (2009) should be cited.

Based on the above mentioned derivations, the Graphene sheet represents an interesting reinforcement for designing multifunctional polymer composites. Graphene-based polymer composites (Ji et al. (2010)) are widely studied using micro-mechanics tools like the scheme by Mori and Tanaka

(1973). However, to derive the effective properties of such composite materials, the Eshelby's tensor for the Graphene sheet accounting for its real geometrical morphology is less discussed and remain a challenging task. Herein, we suggest that the Graphene sheet is not an elliptical inclusion. It is therefore approximated by a rectangular shape. Relevant researches that derive the Eshelby's tensor for an arbitrary inclusion's shape are due to Rodin (1996). He overcomes the resolution of tricky integral equations due by non-uniformity of the strain within non-ellipsoidal inclusions. He therefore derives an algorithmic closed-form solutions of the Eshelby's tensors for arbitrary polygonal and polyhedral inclusions. Moreover, Nozaki and Taya (1997, 2000) highlight that the Eshelby's tensor at the centre and the averaged Eshelby's tensor over a polygonal inclusion are equal to that of a circular inclusion whatever the orientation of the inclusion. Using the irreducible decomposition of the Eshelby's tensor by Zheng et al. (2006), Zou et al. (2010) derive explicit expressions of the Eshelby's Tensor Field (ETF) and its average for a wide variety of non-elliptical inclusions. They formulate some remarks about the elliptical approximation to the average of ETF which is valid for a convex non-elliptical inclusion but becomes unacceptable for a non-convex non-elliptical inclusion. Based on the results of Zou et al. (2010) mainly the averaged Eshelby's tensor, Klusemann et al. (2012) has investigated the effective responses of composites consisting of non-elliptical shape in the context of several homogenisation methods.

The goal of this work is to consider a rectangular inclusion shape for deriving the non-linear elastic effective properties the Graphene sheet-reinforced polymer composite. For such a purpose, the Graphene sheet is considered undergoing non-linear deformations. Therefore, a Taylor series expansion combined with the non-linear stress- strain relationship used in Lee et al. (2008), establishes the expressions of the second order linear elastic and third order non-linear elastic moduli. This enables the derivation of a non-linear constitutive behaviour based on the Modified Morse potential for the Graphene sheet. The irreducible decomposition of the Eshelby's tensor by Zou et al. (2010) and Klusemann et al. (2012) is combined with a rectangular aspect ratio to provide the Graphene sheet with an averaged Eshelby's tensor for homogenisation purposes.

The paper is organised as follows: section 2 establishes the theoretical framework for deriving the non-linear elastic stiffness tensor of the Graphene sheet. In section 3, the procedure for obtaining the Eshelby's tensor for the Graphene sheet is recalled, some numerical calculations are also presented. The Mori-Tanaka micro-mechanics scheme is applied in section 4 leading to the computation of the effective moduli of the composite. Numerical results obtained for different mass fractions are presented and discussed versus the anisotropic degree of the composite.

2. Non-linear stiffness tensor of the Graphene sheet

2.1. Preliminaries on Taylor series expansion

Let us consider a real value function $g(x)$ which is n times differentiable at a real value point x_0 with n being an integer. The Taylor series expansion applied to the function $g(x)$ is given such as:

$$g(x) = \sum_{n=0}^{\infty} \frac{g^{(n)}(x_0)}{n!} (x - x_0)^n \tag{1}$$

Now consider the function $g(x)$ defined as:

$$g(x) = \sqrt{a + bx} \tag{2}$$

where a and b are real constants. The derivatives of the function $g(x)$ for a quadratic truncation are given by:

$$\begin{cases} g(x) = \sqrt{a + bx} \\ g^{'}(x) = \frac{b}{2\sqrt{a+bx}} \\ g^{''}(x) = \frac{b^2}{4(a+bx)\sqrt{a+bx}} \end{cases} \tag{3}$$

Let us $x_0 = 0$, then Eq.(3) can be rewritten as follows:

$$\begin{cases} g(0) = \sqrt{a} \\ g^{'}(0) = \frac{b}{2\sqrt{a}} \\ g^{''}(0) = \frac{b^2}{4a\sqrt{a}} \end{cases} \tag{4}$$

This finally leads to :

$$g(x) = \sqrt{a + bx} \approx \sqrt{a} + \frac{b}{2\sqrt{a}} x - \frac{b^2}{4a\sqrt{a}} x^2 \tag{5}$$

Eq.(5) will be used in section 2.2 to derive the non-linear stiffness tensor for the Graphene sheet.

2.2. *Theoretical framework*

For the Graphene sheet, the experimental force-deformation relation can be expressed as a phenomenological non-linear scalar relation between the applied strain ϵ and the observed stress σ:

$$\sigma = E\epsilon + D\epsilon^2 \tag{6}$$

where E denotes the Young's modulus. It is determined from components of the second-order fourth rank stiffness tensor. D stands for the non-linear (third order) elastic modulus. It is determined from components of both the second-order fourth rank stiffness tensor and the third-order sixth rank stiffness tensor. Rewriting Eq.(6) leads to:

$$f(\epsilon) = D\epsilon^2 + E\epsilon - \sigma = 0 \tag{7}$$

The root of Eq.(7) can be expressed as follows:

$$\epsilon = \frac{-E \pm \sqrt{E^2 + 4D\sigma}}{2D} \tag{8}$$

Considering the general case where $\epsilon > 0$, one gets:

$$\epsilon = \frac{-E + \sqrt{E^2 + 4D\sigma}}{2D} \tag{9}$$

Applying the Taylor series expansion obtained in Eq.(5), it can be obtained for $a = 1$, $b = 4D$, $x = \frac{\sigma}{E^2}$:

$$\sqrt{1 + 4D\frac{\sigma}{E^2}} \approx 1 + \frac{4D}{2}\frac{\sigma}{E^2} - \frac{(4D)^2}{4}\left(\frac{\sigma}{E^2}\right)^2 + 0\left(\left(\frac{\sigma}{E^2}\right)^3\right) \tag{10}$$

Eq.(10) is rewritten as follows:

$$\sqrt{E^2 + 4D\sigma} \approx E + \frac{2D}{E}\sigma - \frac{4D^2}{E^3}\sigma^2 \tag{11}$$

Substituting Eq.(11) into Eq.(9) reads:

$$\epsilon = \frac{1}{E}\sigma - \frac{2D}{E^3}\sigma^2 \tag{12}$$

Assuming that the Graphene sheet is transverse isotropic (i.e in the $x - y$ plane, it is isotropic), let us consider the two tensile conditions for the Graphene sheet under in-plane loading:

- Case 1: $\sigma_x \neq 0$, $\sigma_y = \tau_{xy} = 0$, then;

$$\epsilon_x = \frac{1}{E}\sigma_x - \frac{2D}{E^3}\sigma_x^2; \epsilon_y = \epsilon_z = -\nu\epsilon_x = -\frac{\nu}{E}\sigma_x + \frac{2D\nu}{E^3}\sigma_x^2 \tag{13}$$

where σ_x,σ_y, τ_{xy} are the axial stress and shear stress, respectively, and ν is the Poisson's ratio.

- Case 2: $\sigma_y \neq 0$, $\sigma_x = \tau_{xy} = 0$, then;

$$\epsilon_y = \frac{1}{E}\sigma_y - \frac{2D}{E^3}\sigma_y^2; \epsilon_x = \epsilon_z = -\nu\epsilon_y = -\frac{\nu}{E}\sigma_y + \frac{2D\nu}{E^3}\sigma_y^2 \tag{14}$$

Adding Eq.(13) and Eq.(14), we can obtain:

$$\begin{cases} \epsilon_x = \frac{1}{E}\left(\sigma_x - \nu\sigma_y\right) - \frac{2D}{E^3}\left(\sigma_x^2 - \nu\sigma_y^2\right) \\ \epsilon_y = \frac{1}{E}\left(\sigma_y - \nu\sigma_x\right) - \frac{2D}{E^3}\left(\sigma_y^2 - \nu\sigma_x^2\right) \\ \gamma_{xy} = \frac{2(1+\nu)}{E}\tau_{xy} \end{cases} \tag{15}$$

Rewriting Eq.(15) in a matrix form, one obtains the following expressions:

$$\begin{Bmatrix} \epsilon_x \\ \epsilon_y \\ \gamma_{xy} \end{Bmatrix} = \frac{1}{E}\begin{bmatrix} 1 & -\nu & 0 \\ -\nu & 1 & 0 \\ 0 & 0 & 2\left(1+\nu\right) \end{bmatrix}\begin{Bmatrix} \sigma_x \\ \sigma_y \\ \tau_{xy} \end{Bmatrix} - \frac{2D}{E^3}\begin{bmatrix} 1 & -\nu & 0 \\ -\nu & 1 & 0 \\ 0 & 0 & 0 \end{bmatrix}\begin{Bmatrix} \sigma_x^2 \\ \sigma_y^2 \\ \tau_{xy}^2 \end{Bmatrix} \tag{16}$$

Rearranging Eq.(16) leads to:

$$\begin{cases} \frac{2D}{E^3}\sigma_x^2 - \frac{1}{E}\sigma_x + \frac{1}{1-\nu^2}\left(\epsilon_x + \nu\epsilon_y\right) = 0 \\ \frac{2D}{E^3}\sigma_y^2 - \frac{1}{E}\sigma_y + \frac{1}{1-\nu^2}\left(\epsilon_y + \nu\epsilon_x\right) = 0 \\ \frac{1}{E}\tau_{xy} = \frac{1}{2(1+\nu)}\gamma_{xy} \end{cases} \tag{17}$$

Using the Taylor series expansion from Eq.(11), it can be derived from the first equation of the system.(17):

$$\sigma_x = \frac{\frac{4DE}{1-\nu^2}\left(\epsilon_x + \nu\epsilon_y\right) + \frac{16D^2}{(1-\nu^2)^2}\left(\epsilon_x + \nu\epsilon_y\right)^2}{4D} \tag{18}$$

where we can approximatively obtain for:

$$\left(\epsilon_x + \nu\epsilon_y\right)^2 = \epsilon_x^2 + 2\nu\epsilon_x\epsilon_y + \nu^2\epsilon_y^2 \approx \epsilon_x^2 + \nu^2\epsilon_y^2 \tag{19}$$

Substituting Eq.(19) into Eq.(18), we obtain the non-linear relationship between the stress and strain in the x-direction as:

$$\sigma_x = \frac{E}{1-\nu^2}\left(\epsilon_x + \nu\epsilon_y\right) + \frac{4D}{\left(1-\nu^2\right)^2}\left(\epsilon_x^2 + \nu^2\epsilon_y^2\right) \tag{20}$$

Similarly, the non-linear relationship between the stress and strain in the y-direction is given by:

$$\sigma_y = \frac{E}{1-\nu^2}\left(\epsilon_y + \nu\epsilon_x\right) + \frac{4D}{\left(1-\nu^2\right)^2}\left(\epsilon_y^2 + \nu^2\epsilon_x^2\right) \tag{21}$$

Rewriting Eq.(20), Eq.(21) and the third equation of Eq.(15) in a matrix form, the non-linear stiffness tensor yields the following expressions:

$$\left\{\begin{array}{c}\sigma_x\\ \sigma_y\\ \tau_{xy}\end{array}\right\} = \frac{E}{1-\nu^2}\begin{bmatrix}1 & \nu & 0\\ \nu & 1 & 0\\ 0 & 0 & \frac{1-\nu}{2}\end{bmatrix}\left\{\begin{array}{c}\epsilon_x\\ \epsilon_y\\ \gamma_{xy}\end{array}\right\} + \frac{4D}{\left(1-\nu^2\right)^2}\begin{bmatrix}1 & \nu^2 & 0\\ \nu^2 & 1 & 0\\ 0 & 0 & 0\end{bmatrix}\left\{\begin{array}{c}\epsilon_x^2\\ \epsilon_y^2\\ \gamma_{xy}^2\end{array}\right\} \tag{22}$$

Let $\mathbf{L}_g$ denotes the matrix form of the linear stiffness tensor and $\mathbf{N}_g$ that of the non-linear stiffness tensor, then we can obtain:

$$\{\boldsymbol{\sigma}\} = \mathbf{L}_g\{\boldsymbol{\epsilon}\} + \mathbf{N}_g\left\{\boldsymbol{\epsilon}^2\right\} \tag{23}$$

where $\mathbf{L}_g$ and $\mathbf{N}_g$ are expressed as:

$$\mathbf{L}_g = \frac{E}{1-\nu^2}\begin{bmatrix}1 & \nu & 0\\ \nu & 1 & 0\\ 0 & 0 & \frac{1-\nu}{2}\end{bmatrix};\ \mathbf{N}_g = \frac{4D}{\left(1-\nu^2\right)^2}\begin{bmatrix}1 & \nu^2 & 0\\ \nu^2 & 1 & 0\\ 0 & 0 & 0\end{bmatrix} \tag{24}$$

2.3. *Evaluation of elastic moduli of the Graphene sheet*

In molecular mechanics, the total potential energy of the Graphene sheet can be expressed as a sum of several energy terms as proposed by Cho et al. (2007). Under in-plane loading (Fig.1), the modified Morse potential function and its constants were adopted to describe the elastic behaviour. They are given as follows by Xiao et al. (2005); Cho et al. (2007):

$$U_{in-plane} = D\left\{\left[1-e^{-\beta(\Delta r)}\right]^2 - 1\right\} + \frac{1}{2}k_{\theta_1}\left(\Delta\theta\right)^2\left[1 + k_{\theta_2}\left(\Delta\theta\right)^4\right] \tag{25}$$

where $D = 0.6031nN.nm$, $\beta = 26.25nm^{-1}$, $k_{\theta_1} = 1.42nN.nm/rad^2$, and $k_{\theta_2} = 0.754rad^{-4}$; Δr is the variation of bonding length between bonded carbon atoms; $\Delta\theta$ is the variation of the angle formed by three neighbouring atoms.The force-deformation response of the Graphene sheet can be analysed with the representative elements shown in Fig.1. The forces and moments acting on the atoms are obtained from their relative displacements such as Xiao et al. (2005); Cho et al. (2007):

$$\left\{\begin{array}{l} F\left(\Delta r\right) = \frac{\partial U_{in-plane}}{\partial\Delta r} = 2\beta D\left(1-e^{-\beta(\Delta r)}\right)e^{-\beta(\Delta r)}\\ M\left(\Delta\theta\right) = \frac{\partial U_{in-plane}}{\partial\Delta\theta} = k_{\theta_1}\Delta\theta + 3k_{\theta_1}k_{\theta_2}\left(\Delta\theta\right)^5 \approx k_{\theta_1}\Delta\theta\end{array}\right. \tag{26}$$

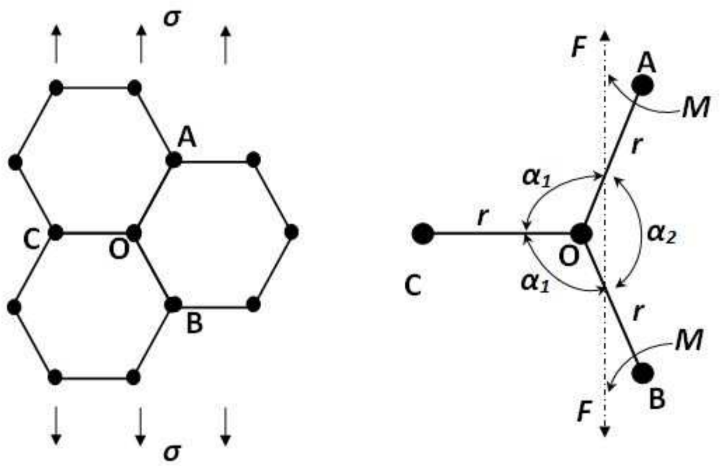

Figure 1: Representative elements of a Graphene sheet under tensile loading as proposed by Xiao et al. (2005).

For uni-axial tension in the 1-direction in Fig.1, the equilibrium condition is written following Cho et al. (2007):

$$\frac{r}{2}F\left(\Delta r\right) = \tan\left(\frac{\alpha_2}{2}\right)\left[M\left(\Delta\alpha_2\right) - M\left(\Delta\alpha_1\right)\right] \tag{27}$$

where r is the bond length ($r = 0.142nm$), Δr is the variation of the bond length; α_2 is the angle of the carbon bonds ($\alpha_2 = 120°$); $\Delta\alpha_1$ and $\Delta\alpha_2$ are the angle variations of the bonds which are related as follows:

$$\Delta\alpha_2 = -2\Delta\alpha_1 \tag{28}$$

The relationship between the bond-length and the bond angle variation is written as:

$$\Delta\alpha_2 = \frac{2r\left[\beta D\left(1 - e^{-\beta(\Delta r)}\right)e^{-\beta(\Delta r)}\right]}{3k_{\theta_1}\tan\left(\frac{\alpha_2}{2}\right)} = \left(\frac{2r}{3}\right)\frac{\beta D\left(1 - e^{-\beta(\Delta r)}\right)e^{-\beta(\Delta r)}}{k_{\theta_1}}\cot\left(\frac{\alpha_2}{2}\right) \tag{29}$$

From Eqs.(26)- (29), we can obtain the in-plane axial stress σ_{11} and strains ϵ_{11}, ϵ_{22} as:

$$\sigma_{11} = \frac{F\left(\Delta r\right)}{tr\sin\left(\frac{\alpha_2}{2}\right)\left(1 + \cos\left(\frac{\alpha_2}{2}\right)\right)} \tag{30}$$

with t the thickness of the Graphene sheet ($t = 0.335nm$).

$$\epsilon_{11} = \frac{\Delta r\sin\left(\frac{\alpha_2}{2}\right) + \frac{r}{2}\cos\left(\frac{\alpha_2}{2}\right)\Delta\alpha_2}{r\sin\left(\frac{\alpha_2}{2}\right)} \tag{31}$$

$$\epsilon_{22} = \frac{\Delta r\cos\left(\frac{\alpha_2}{2}\right) - \frac{r}{2}\sin\left(\frac{\alpha_2}{2}\right)\Delta\alpha_2}{r + r\cos\left(\frac{\alpha_2}{2}\right)} \tag{32}$$

One can notice that:

$$\Delta r = \epsilon r \tag{33}$$

Substituting Eq. (33) and Eq. (26) into Eq. (30), the expression of in-plane axial stress is given by:

$$\sigma_{11} = \frac{2\beta D}{tr \sin\left(\frac{\alpha_2}{2}\right)\left(1+\cos\left(\frac{\alpha_2}{2}\right)\right)}\left(1-e^{-\beta r\epsilon}\right)e^{-\beta r\epsilon} \tag{34}$$

Assuming a non-linear relationship between the in-plane stress and strain, one gets:

$$\sigma_{11} = E_g\epsilon + D_g\epsilon^2 \tag{35}$$

where, E_g and D_g are the linear elastic modulus and non-linear elastic modulus of the Graphene sheet. Comparing Eq. (34) and Eq. (35), we can obtain:

$$E_g\epsilon + D_g\epsilon^2 = \frac{2\beta D}{tr \sin\left(\frac{\alpha_2}{2}\right)\left(1+\cos\left(\frac{\alpha_2}{2}\right)\right)}\left(1-e^{-\beta r\epsilon}\right)e^{-\beta r\epsilon} \tag{36}$$

where β, D, t, r, α_2 are all constant values. Given two different strain values ϵ_a and ϵ_b, the linear elastic modulus E_g and non-linear elastic modulus D_g can be calculated as:

$$\left\{\begin{array}{c} E_g \\ D_g \end{array}\right\} = \frac{2\beta D}{tr \sin\left(\frac{\alpha_2}{2}\right)\left(1+\cos\left(\frac{\alpha_2}{2}\right)\right)}\begin{bmatrix} \epsilon_a & \epsilon_a^2 \\ \epsilon_b & \epsilon_b^2 \end{bmatrix}^{-1}\left\{\begin{array}{c} \left(1-e^{-\beta r\epsilon_a}\right)e^{-\beta r\epsilon_a} \\ \left(1-e^{-\beta r\epsilon_b}\right)e^{-\beta r\epsilon_b} \end{array}\right\} \tag{37}$$

If the strain is greater than the critical strain ϵ_{cr} corresponding to the maximum stress, the structure is not stable, so let $\epsilon_a = \epsilon_{cr}$. When the strain is small, the relationship between the stress and strain appear linear. According to relevant data from Morse potential (Xiao et al. (2005); Cho et al. (2007)), one has $\epsilon_a = 0.05$ leading to $\sigma_a = 72.3\ GPa$ and $\epsilon_{cr} = 0.185$ leading to $\sigma_{cr} = 128\ GPa$. So let $\epsilon_b = 0.05$. Substituting ϵ_a, ϵ_b and relevant parameters into Eq.(37), the linear elastic modulus E_g and non-linear elastic modulus D_g are calculated as:

$$\begin{cases} E_g = 1557.32\ GPa \\ D_g = -4594.93\ GPa \end{cases} \tag{38}$$

The difference between the calculated values and fitted values is depicted by Fig. 2. The fitted values are given such as:

$$\sigma = E_g\epsilon + D_g\epsilon^2 = 1557.32\epsilon - 4594.93\epsilon^2\ (GPa) \tag{39}$$

Based on the fitted values, the maximum stress is about $\sigma_{cr} = 132\ GPa$ and $\epsilon_{cr} = 0.17$ as shown by Fig. 2. The relative error with respect to the Morse potential curve is about 3% for σ_{cr} and 8%

References	E [TPa]	ν	D [TPa]
Lee et al. (2008)$^{(a)}$	1.0	0.165	-2.0
Cho et al. (2007)$^{(b)}$	1.156	0.195	-
Xiao et al. (2005)$^{(c)}$	1.13	0.2	-
Cadelano et al. (2009)$^{(d)}$	0.931	0.31	-1.74$^{(e)}$
			-3.137$^{(f)}$
Lee et al. (2012)$^{(g)}$	2.4	0.16	-
Present study	1.55	0.2	-4.594

Table 1: In-plane comparison of elastic constants of the Graphene sheet with thickness $t = 0.335\ nm$. (a)NanoIndentation AFM, (b) Modified Morse and Lennard Jones potentials, (c) Modified Morse potential, (d) Continuum elasticity and Tight binding simulation, (e) small strain, (f) Lagragian strain, (g) Raman spectroscopy.

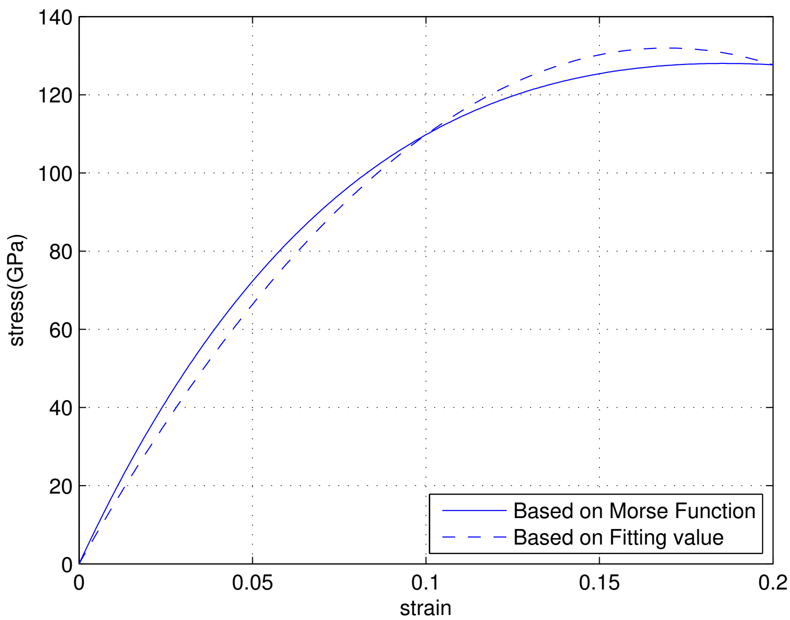

Figure 2: Stress-strain curve of graphene sheet.

for ϵ_{cr}.

Using Eq.(31) and Eq.(32), the Poisson's ratio ν yields:

$$\nu = -\frac{\epsilon_{22}}{\epsilon_{11}} = \frac{r\sin\left(\frac{\alpha_2}{2}\right)\left[\Delta r\cos\left(\frac{\alpha_2}{2}\right) - \frac{r}{2}\sin\left(\frac{\alpha_2}{2}\right)\Delta\alpha_2\right]}{\left[r + r\cos\left(\frac{\alpha_2}{2}\right)\right]\left[\Delta r\sin\left(\frac{\alpha_2}{2}\right) + \frac{r}{2}\cos\left(\frac{\alpha_2}{2}\right)\Delta\alpha_2\right]} \tag{40}$$

Substituting relevant parameters into Eq.(40), the relationship between the strain and the Poisson's ratio is shown by Fig.3. Using the Fitting method, we can obtain:

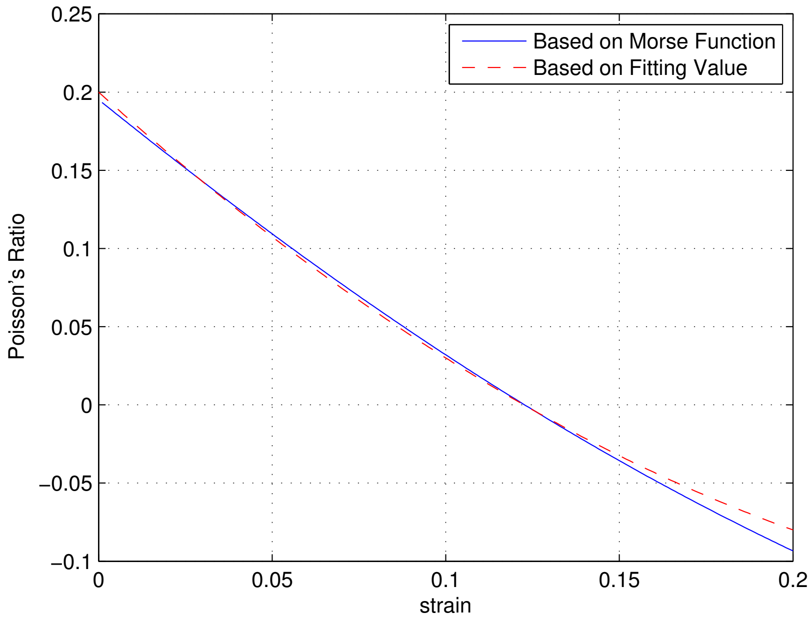

Figure 3: Poisson's ratio versus strain curve of graphene sheet.

$$\nu \approx 0.2 - 2\epsilon + 3\epsilon^2 \approx 0.2 \tag{41}$$

Table 1 compares the present predictions along with data from the open literature. The observed difference between values in Table 1 can be explained by the large variation of these properties among published data from experimental and theoretical studies due to the use of different potential functions based on different algorithms. Substituting the value of Eq.(38) and Eq.(41) into Eq.(24), the linear stiffness tensor $\mathbf{L}_g$ and the non-linear stiffness tensor $\mathbf{N}_g$ yield values of Table 2.

Lg_{1111}	Lg_{2222}	Lg_{1212}	Lg_{1122}	Lg_{1112}	Lg_{2212}
1622.21	1622.21	648.88	324.44	0.0	0.0
Ng_{1111}	Ng_{2222}	Ng_{1212}	Ng_{1122}	Ng_{1112}	Ng_{2212}
-18379.72	-18379.72	0.0	-735.19	0.0	0.0

Table 2: Components in [GPa] of the linear and non-linear stiffness tensors $\mathbf{L}_g$ and $\mathbf{N}_g$

3. Eshelby's tensor for the Graphene sheet reinforcement

3.1. Eshelby's tensor for general shape inclusions

For two-dimensional isotropic material, the averaged Eshelby's tensor for an arbitrary inclusion shape is expressed by Zou et al. (2010):

$$\mathbf{S} = \mathbf{S}_0 + \mathbf{S}_\omega \tag{42}$$

where $\mathbf{S}_0$ denotes the Eshelby's tensor of an unit circle whereas $\mathbf{S}_\omega$ stands for the Eshelby's tensor of intersection parts between the inclusion boundaries and the unit circle. Based on the results by Mura (1991), $\mathbf{S}_0$ is equal to the Eshelby's tensor for a circular inclusion such as:

$$\mathbf{S}_0 = \frac{1}{8(1-\nu)} \begin{bmatrix} 5-4\nu & 4\nu-1 & 0 \\ 4\nu-1 & 5-4\nu & 0 \\ 0 & 0 & 3-4\nu \end{bmatrix} \tag{43}$$

Following works by Zou et al. (2010), the average of the anisotropic part of the Eshelby's tensor is given by:

$$\mathbf{S}_\omega = \frac{1}{(1-\nu)} \begin{bmatrix} (1-\nu)p_2 + p_4 & \nu p_2 - p_4 & \frac{(1-2\nu)}{2} q_2 + q_4 \\ -\nu p_2 - p_4 & -(1-\nu)p_2 + p_4 & \frac{(1-2\nu)}{2} q_2 - q_4 \\ \frac{1}{2} q_2 + q_4 & \frac{1}{2} q_2 - q_4 & -p_4 \end{bmatrix} \tag{44}$$

where p_2, q_2, p_4 and q_4 are derived from the following complex-variable of boundary integrals such as:

$$\begin{cases} \gamma_2(x) = p_2(x) + \mathbf{i}q_2(x) = -\frac{1}{8\pi\omega} \oint_{\partial\omega} \oint_{\partial\omega} \frac{z}{\bar{z}} dy d\bar{x} \\ \gamma_4(x) = p_4(x) + \mathbf{i}q_4(x) = -\frac{1}{32\pi\omega} \oint_{\partial\omega} \oint_{\partial\omega} \frac{z}{\bar{z}} dy dx \end{cases} \tag{45}$$

with $\mathbf{i}$ the unit imaginary number, $x = x_1 + \mathbf{i}x_2$, $y = y_1 + \mathbf{i}y_2$ and $z = y - x$ are the complex representations of the position vectors x, y and relative position vector $z = y - x$. $(\bar{\bullet})$ stands for the complex conjugation.

3.2. *Eshelby's tensor for a rectangular inclusion*

Let us consider a rectangular inclusion of size $(2a \times 2b)$ with $a \geq b$. For easiness of calculation, let us assume that $(a^2 + b^2 = 1)$. As illustrated in Fig.4, the longer and shorter sides are set to be parallel to the orthonormal basis vectors i_1 and i_2, respectively. The coordinates of the four vertices

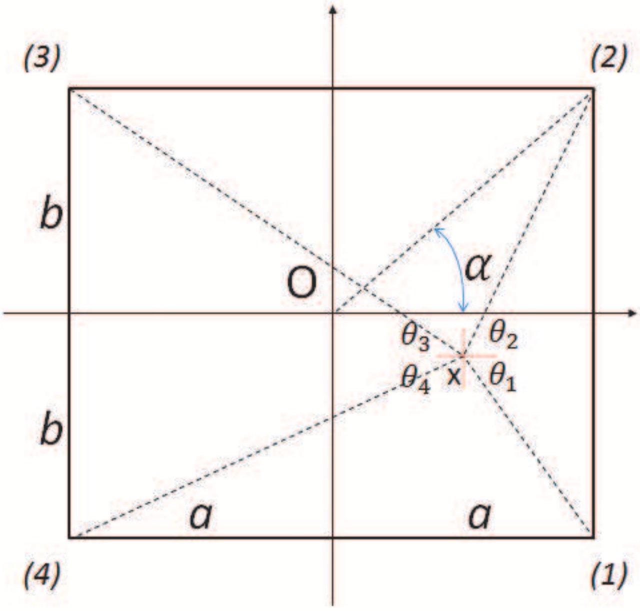

Figure 4: Geometric parameter of rectangular inclusion.

are expressed by:

$$\begin{cases} y_{(1)} = e^{-\mathbf{i}\alpha} \\ y_{(2)} = e^{\mathbf{i}\alpha} \\ y_{(3)} = e^{\mathbf{i}(\pi-\alpha)} \\ y_{(4)} = e^{\mathbf{i}(\pi+\alpha)} \end{cases} \tag{46}$$

where $\alpha = \arctan\left(\frac{b}{a}\right)$. Let us introduce the local geometric parameters like:

$$\begin{cases} \theta_1 = -\arg\left[z_{(1)}\right] \\ \theta_2 = \arg\left[z_{(2)}\right] \\ \theta_3 = \pi - \arg\left[z_{(3)}\right] \\ \theta_4 = \pi + \arg\left[z_{(4)}\right] \end{cases} \tag{47}$$

with $\theta_i\,(i = 1, 2, 3, 4) \in \left[0, \frac{\pi}{2}\right]$ for all interior points. Thus:

$$\begin{cases} \gamma_2 = \frac{2}{\pi}\left(\arctan\eta - \frac{\pi}{4}\right) - \frac{1}{2\pi\eta}\ln\left(1+\eta^2\right) + \frac{1}{2\pi}\ln\left(\frac{1+\eta^2}{\eta^2}\right) \\ \gamma_4 = -\frac{1}{8} + \frac{1}{4\pi\eta}\ln\left(1+\eta^2\right) + \frac{\eta}{4\pi}\ln\left(\frac{1+\eta^2}{\eta^2}\right) \end{cases} \tag{48}$$

where η is the aspect ratio such as $\eta = \frac{b}{a}$; $\eta \leq 1$. Based on Eq.(48) and Eq.(45), one gets for p_2, q_2, p_4 and q_4 the following expressions:

$$\begin{cases} p_2 = \frac{2}{\pi}\left(\arctan\eta - \frac{\pi}{4}\right) - \frac{1}{2\pi\eta}\ln\left(1+\eta^2\right) + \frac{1}{2\pi}\ln\left(\frac{1+\eta^2}{\eta^2}\right) \\ q_2 = 0 \\ p_4 = -\frac{1}{8} + \frac{1}{4\pi\eta}\ln\left(1+\eta^2\right) + \frac{\eta}{4\pi}\ln\left(\frac{1+\eta^2}{\eta^2}\right) \\ q_4 = 0 \end{cases} \tag{49}$$

Finally, the averaged Eshelby's tensor $\mathbf{S}_\omega$ is obtained by substituting Eq.(49) into Eq.(44).

From Eq.(41), the Poisson's ratio ν of the Graphene sheet is about 0.2. Substituting this value into Eq.(43), we can obtain the value of $\mathbf{S}_0$ as shown in Table3. Let $\eta = [0.2, 0.4, 0.6, 0.8, 1]$. Using Eqs.(42)-(44) and Eq.(49), we get in Table4 the Eshelby's tensor of a rectangular Graphene-sheet inclusion for different aspect ratio η.

S_{1111}	S_{2222}	S_{1212}	S_{1122}	S_{2211}	S_{1112}	S_{1211}	S_{2212}	S_{1222}
0.6563	0.6563	0.3438	-0.0312	-0.0312	0.0	0.0	0.0	0.0

Table 3: Components of the Eshelby's tensor $\mathbf{S}_0$ for a circular inclusion.

η	S_{1111}	S_{2222}	S_{1212}	S_{1122}	S_{2211}	S_{1112}	S_{1211}	S_{2212}	S_{1222}
0.2	0.2825	0.8862	0.4157	-0.0348	0.1161	0.0	0.0	0.0	0.0
0.4	0.4250	0.8064	0.3843	-0.0384	0.0569	0.0	0.0	0.0	0.0
0.6	0.5197	0.7409	0.3697	-0.0330	0.0223	0.0	0.0	0.0	0.0
0.8	0.5873	0.6854	0.3636	-0.0237	0.0009	0.0	0.0	0.0	0.0
1.0	0.6379	-0.6379	0.3621	-0.0129	-0.0129	0.0	0.0	0.0	0.0

Table 4: Components of the Eshelby's tensor $\mathbf{S}$ versus the aspect ratio η.

4. Effective elastic moduli of the Graphene sheet-reinforced composite

4.1. Theoretical analysis

In this paper, we assume that the Graphene sheet inclusions are ideally distributed in the polymer matrix. The Mori-Tanaka micro-mechanics scheme is adopted to predict the effective response of the composite. The Mori-Tanaka method considers that each inclusion is embedded in an infinite matrix subjected to the averaged stress $\boldsymbol{\sigma}_m$ or averaged strain $\boldsymbol{\epsilon}_m$ of the matrix. According to the Eshelby's equivalent inclusion theory, the averaged strain $\boldsymbol{\epsilon}_g$ of the Graphene sheet inclusion is given by:

$$\boldsymbol{\epsilon}_g = \mathbf{A}_g \boldsymbol{\epsilon}_m \tag{50}$$

where $\mathbf{A}_g$ is the strain concentration tensor given by:

$$\mathbf{A}_g = \left[\mathbf{I} + \mathbf{S}\mathbf{L}_m^{-1} \left(\mathbf{L}_g - \mathbf{L}_m\right)\right]^{-1} \tag{51}$$

with $\mathbf{I}$ and $\mathbf{S}$ denoting the identity tensor and the Eshelby's tensor, respectively. Let us assume that the averaged stress and strain tensor of the Graphene sheet-reinforced polymer composite are $\bar{\boldsymbol{\sigma}}$ and $\bar{\boldsymbol{\epsilon}}$. They are given by:

$$\bar{\boldsymbol{\sigma}} = \frac{1}{V} \int_V \boldsymbol{\sigma} dV = V_g \boldsymbol{\sigma}_g + V_m \boldsymbol{\sigma}_m \tag{52}$$

$$\bar{\boldsymbol{\epsilon}} = \frac{1}{V} \int_V \boldsymbol{\epsilon} dV = V_g \boldsymbol{\epsilon}_g + V_m \boldsymbol{\epsilon}_m \tag{53}$$

where V_g and V_m denote the volume fraction of the Graphene sheet reinforcement and that of the matrix, respectively. One gets $(V_g + V_m = 1)$. Also the local stress within the Graphene sheet and the matrix are given by:

$$\begin{cases} \boldsymbol{\sigma}_g = \mathbf{L}_g \boldsymbol{\epsilon}_g + \mathbf{N}_g \boldsymbol{\epsilon}_g^2 \\ \boldsymbol{\sigma}_m = \mathbf{L}_m \boldsymbol{\epsilon}_g \end{cases} \tag{54}$$

Substituting Eqs.(54) and (50) into Eq.(52), we obtain:

$$\bar{\boldsymbol{\sigma}} = \left(V_g \mathbf{L}_g \mathbf{A}_g + V_m \mathbf{L}_m\right) \boldsymbol{\epsilon}_m + V_g \mathbf{N}_g \mathbf{A}_g^2 \boldsymbol{\epsilon}_m^2 \tag{55}$$

The non-linear relationship between the stress and the strain for the homogenised Graphene sheet-reinforced polymer composite is defined by:

$$\bar{\boldsymbol{\sigma}} = \mathbf{L}\bar{\boldsymbol{\epsilon}} + \mathbf{N}\bar{\boldsymbol{\epsilon}}^2 \tag{56}$$

where $\mathbf{L}$ and $\mathbf{N}$ are the effective linear and non-linear stiffness tensors of the composite. Substituting Eqs.(53) and (50) into Eq.(56), the averaged stress yields:

$$\bar{\boldsymbol{\sigma}} = \mathbf{L}\left(V_g \mathbf{A}_g + V_m \mathbf{I}\right) \boldsymbol{\epsilon}_m + \mathbf{N}\left(V_g^2 \mathbf{A}_g^2 + 2 V_g V_m \mathbf{A}_g + V_m^2 \mathbf{I}\right) \boldsymbol{\epsilon}_m^2 \tag{57}$$

By comparing Eq.(55) and Eq.(57) , we express tensors $\mathbf{L}$ and $\mathbf{N}$ of the Graphene sheet-reinforced polymer composite as:

$$\begin{cases} \mathbf{L} = \left(V_g \mathbf{L}_g \mathbf{A}_g + V_m \mathbf{L}_m\right)\left(V_g \mathbf{A}_g + V_m \mathbf{I}\right)^{-1} \\ \mathbf{N} = V_g \mathbf{N}_g \mathbf{A}_g^2 \left(V_g^2 \mathbf{A}_g^2 + 2V_g V_m \mathbf{A}_g + V_m^2 \mathbf{I}\right)^{-1} \end{cases} \tag{58}$$

Let us consider a composite consisting of the Graphene sheet and the matrix. The following symbol notation $m_{c,g,m}$ is stated for the mass of composite, the Graphene sheet, and the polymer matrix, respectively. The mass fractions of the Graphene sheet M_g and the matrix M_m are defined as:

$$M_g = \frac{m_g}{m_c};\; M_m = \frac{m_m}{m_c} \tag{59}$$

The relationship between the mass fraction and the volume fraction is obtained such as:

$$M_g = \frac{\rho_g}{\rho_g V_g + \rho_m V_m} V_g;\; M_m = \frac{\rho_m}{\rho_g V_g + \rho_m V_m} V_m \tag{60}$$

or

$$V_g = \frac{\rho_m}{\rho_g M_m + \rho_m M_g} M_g;\; V_m = \frac{\rho_g}{\rho_g M_m + \rho_m M_g} M_m \tag{61}$$

where $(\rho_{c,g,m})$ denotes the density of the composite, Graphene, and that of the matrix, respectively. Typical properties of the Graphene sheet and the epoxy polymer are presented in Table 5.

Properties	Graphene sheet	Epoxy polymer matrix
Elastic modulus	$E_g = 1557.32\ GPa$	$E_m = 2\ GPa$
	$D_g = -4594.93\ GPa$	
Poisson's ratio	$\nu_g = 0.2$	$\nu_m = 0.39$
Density	$\rho_g = 1.06\ g/cm^3$	$\rho_m = 1.13\ g/cm^3$

Table 5: Phase properties for the Graphene sheet-reinforced composite.

4.2. Discussion of results

Using the values of Table 5, Table2and Table4, Eq.(51) and Eq.(58), the linear stiffness tensor $\mathbf{L}$ and the non-linear stiffness tensor $\mathbf{N}$ of the Graphene sheet-reinforced polymer composite are computed for different mass fractions. Different aspect ratios η are analysed. The results are

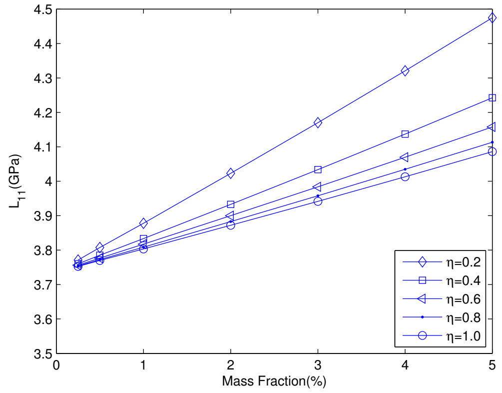

(a) L_{11}

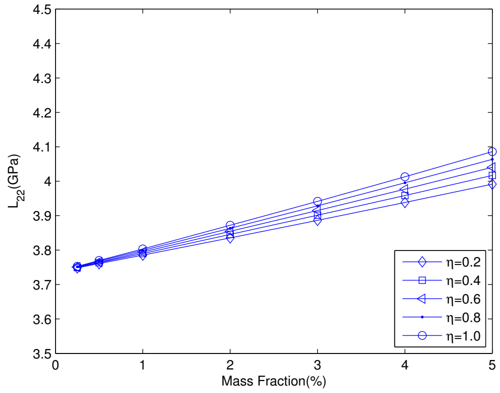

(b) L_{22}

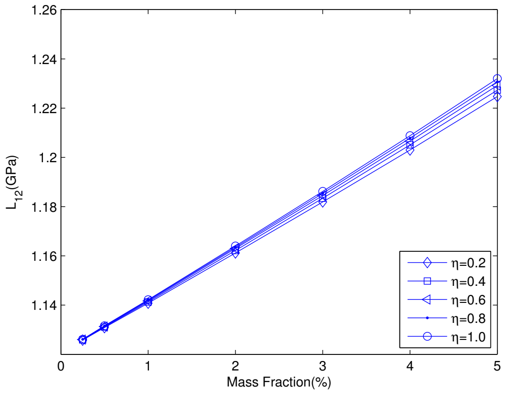

(c) L_{12}

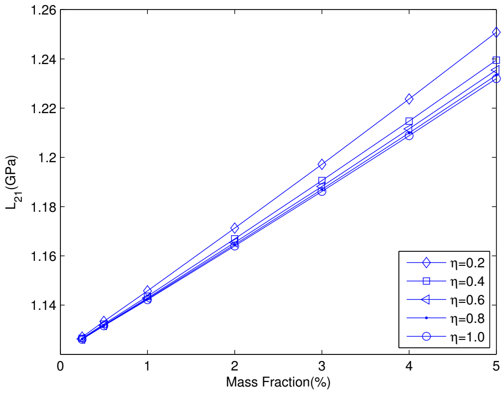

(d) L_{21}

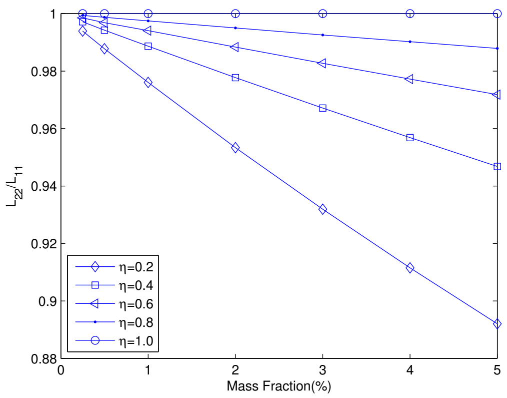

(e) L_{22}/L_{11}

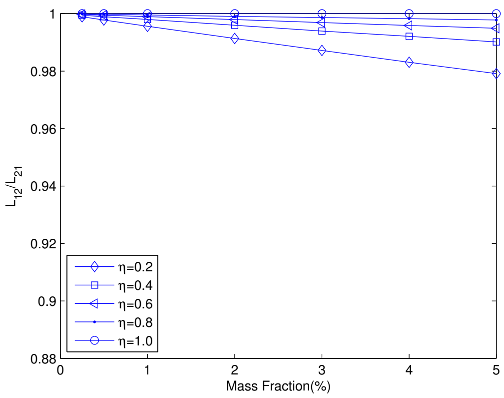

(f) L_{12}/L_{21}

Figure 5: Components of the effective linear stiffness tensor **L** versus the mass fraction.

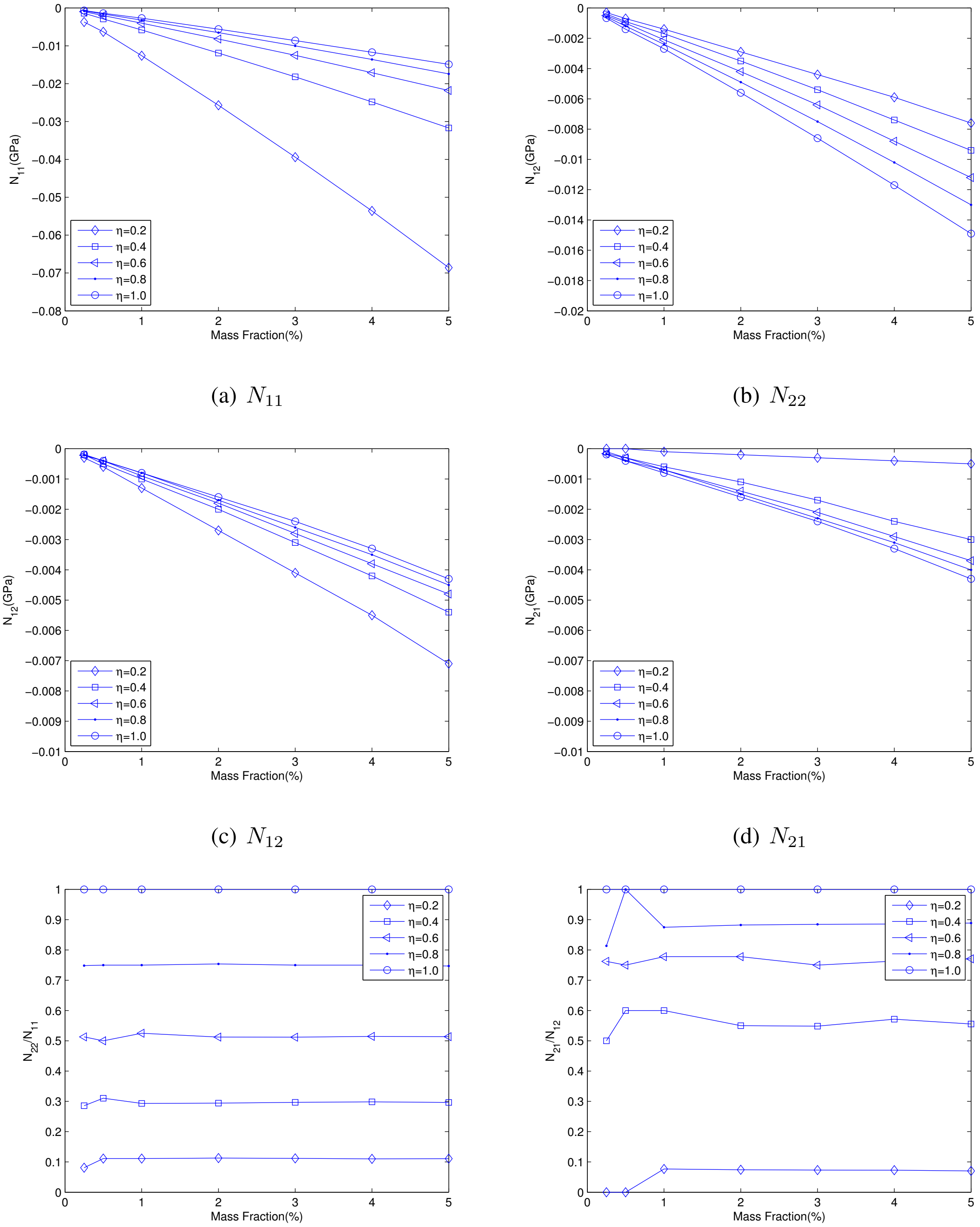

(a) N_{11} (b) N_{22}

(c) N_{12} (d) N_{21}

(e) N_{22}/N_{11} (f) N_{21}/N_{12}

Figure 6: Components of the effective non-linear stiffness tensor **N** versus the mass fraction.

presented in Appendix A. Fig.5 and Fig.6 depict the effective response of the composite versus the mass fraction and thus for different aspect ratio ($\eta = [0.2, 0.4, 0.6, 0.8, 1.0]$). Components of the linear stiffness tensor **L** are depicted in Fig.5 where an increase of L_{11}, L_{22}, L_{12}, L_{21} is observed with the evolution of the mass fraction. However a decrease of the elastic modulus L_{11} and L_{21} (Fig.5-a and Fig.5-d) from thin rectangular shape ($\eta = 0.2$) to square-like shape ($\eta = 1$) is noticed regarding to η. Fig.5-b and Fig.5-c present opposite trends for L_{22} and L_{12} where an increase from thin rectangular shape ($\eta = 0.2$) to square-l ike shape ($\eta = 1$) is observed for the composite. Also, the anisotropic degree is analysed through Fig.5-e and Fig.5-f. In both case, the material properties is nearly symmetric and the isotropic behaviour is shown for high value of η i.e nearly square inclusions.

Results in Fig.6 show a decrease of the components N_{11}, N_{22}, N_{12}, N_{21} versus the evolution of the mass fraction. With respect to η, similar trends are noticed for N_{11}, and N_{12}. An increase is observed from ($\eta = 0.2$) to ($\eta = 1$) as shown by Fig.6-a and Fig.6-c. However, high value of η results a decrease of components N_{22}, and N_{21}. Finally the anisotropy is analysed. Results in Fig.6-e and Fig.6-f show that the non-linear stiffness tensor is fully anisotropic for low value of η. This anisotropy decreases when η increases. An isotropic behaviour is noticed for $\eta = 1$ corresponding to square-like shape.

5. Conclusion

The non-linear effective behaviour has been studied for the Graphene sheet-polymer composite throughout this work. The determination of elastic properties of the Graphene sheet is carried out using an approach that combines a Taylor expansion in power of strains and the modified Morse potential. Therefore values are obtained for the linear elastic modulus Eg and the non-linear elastic modulus Dg of the Graphene sheet. To determine the overall properties, the Eshelby's tensor for an arbitrary inclusion shape is considered through the irreducible decomposition. Especially, the Eshelby's tensor for a rectangular aspect ratio η is analysed for the Graphene sheet inclusion. Several aspect ratio such as ($\eta = [0.2, 0.4, 0.6, 0.8, 1.0]$) are selected for homogenisation under the Mori-Tanaka micro-mechanics scheme. So, the effective linear stiffness tensor **L** and effective non-linear stiffness tensor **N** are obtained for different mass fractions. The results indicate that **L** is enhanced with the increase of mass fractions whereas a decrease is observed for **N**. The results also show that the degree of anisotropy is decrease with the increase of the aspect ratio. For all range of mass fractions, the square-like shape is shown to gather an isotropic behaviour for both the linear and non-linear stiffness tensors. This theoretical study may help to understand the non-linear behaviour of the Graphene sheet-reinforced polymer composites and to model and analyse the non-linear properties of Graphene-based composites.

6. Acknowledgements

The research leading to these results has received funding from the European Union Seventh Framework Programme under grant agreement No. **604391 Graphene Flagship**.

Appendix A. Effective moduli versus different mass fractions

η	$M_g(\%)$	L_{11}	L_{22}	L_{12}	L_{21}	N_{11}	N_{22}	N_{12}	N_{21}
0.2	0.25	3.7711	3.7483	1.1258	1.1270	-0.0031	-0.0003	-0.0003	-0.0000
	0.5	3.8074	3.7609	1.1309	1.1334	-0.0063	-0.0007	-0.0006	-0.0000
	1	3.8781	3.7853	1.1408	1.1458	-0.0126	-0.0014	-0.0013	-0.0001
	2	4.0231	3.8355	1.1612	1.1713	-0.0257	-0.0029	-0.0027	-0.0002
	3	4.1702	3.8863	1.1819	1.1972	-0.0394	-0.0044	-0.0041	-0.0003
	4	4.3207	3.9384	1.2030	1.2237	-0.0536	-0.0059	-0.0055	-0.0004
	5	4.4748	3.9917	1.2247	1.2508	-0.0686	-0.0076	-0.0071	-0.0005
0.4	0.25	3.7601	3.7495	1.1259	1.1265	-0.0014	-0.0004	-0.0001	-0.0001
	0.5	3.7850	3.7633	1.1311	1.1323	-0.0029	-0.0009	-0.0005	-0.0003
	1	3.8335	3.7901	1.1413	1.1436	-0.0580	-0.0017	-0.0010	-0.0006
	2	3.9329	3.8453	1.1622	1.1669	-0.0119	-0.0035	-0.0020	-0.0011
	3	4.0337	3.9012	1.1834	1.1906	-0.0182	-0.0054	-0.0031	-0.0017
	4	4.1369	3.9584	1.2051	1.2147	-0.0248	-0.0074	-0.0042	-0.0024
	5	4.2425	4.0169	1.2273	1.2395	-0.0317	-0.0094	-0.0054	-0.0030
0.6	0.25	3.7561	3.7506	1.1260	1.1263	-0.9743×10^{-3}	-0.4999×10^{-3}	-0.2155×10^{-3}	-0.1643×10^{-3}
	0.5	3.7768	3.7656	1.1313	1.1319	-0.0020	-0.0010	-0.0004	-0.0003
	1	3.8172	3.7947	1.1417	1.1429	-0.0040	-0.0021	-0.0009	-0.0007
	2	3.8999	3.8545	1.1630	1.1654	-0.0082	-0.0042	-0.0018	-0.0014
	3	3.9839	3.9151	1.1845	1.1882	-0.0125	-0.0064	-0.0025	-0.0021
	4	4.0698	3.9771	1.2066	1.2116	-0.0171	-0.0088	-0.0038	-0.0029
	5	4.1577	4.0406	1.2292	1.2355	-0.0218	-0.0112	-0.0048	-0.0037
0.8	0.25	3.7540	3.7517	1.1261	1.1262	-0.7762×10^{-3}	-0.5809×10^{-3}	-0.2205×10^{-3}	-0.1794×10^{-3}
	0.5	3.7726	3.7678	1.1315	1.1317	-0.0016	-0.0012	-0.0004	-0.0004
	1	3.8086	3.7991	1.1420	1.1425	-0.0032	-0.0024	-0.0008	-0.0007
	2	3.8827	3.8634	1.1635	1.1646	-0.0065	-0.0049	-0.0017	-0.0015
	3	3.9578	3.9285	1.1854	1.1870	-0.0100	-0.0075	-0.0026	-0.0023
	4	4.0346	3.9953	1.2078	1.2099	-0.0136	-0.0102	-0.0035	-0.0031
	5	4.1133	4.0635	1.2307	1.2334	-0.0174	-0.0130	-0.0045	-0.0040
1.0	0.25	3.7528	3.7528	1.1261	1.1261	-0.6653×10^{-3}	-0.6653×10^{-3}	-0.1899×10^{-3}	-0.1899×10^{-3}
	0.5	3.7699	3.7699	1.1316	1.1316	-0.0014	-0.0014	-0.0004	-0.0004
	1	3.8034	3.8034	1.1422	1.1422	-0.0027	-0.0027	-0.0008	-0.0008
	2	3.8721	3.8721	1.1640	1.1640	-0.0056	-0.0056	-0.0016	-0.0016
	3	3.9417	3.9417	1.1862	1.1862	-0.0086	-0.0086	-0.0024	-0.0024
	4	4.0130	4.0130	1.2088	1.2088	-0.0117	-0.0117	-0.0033	-0.0033
	5	4.0859	4.0859	1.2320	1.2320	-0.0149	-0.0149	-0.0043	-0.0043

Table A.6: Effective moduli [GPa] versus mass fractions.

References

Cadelano, E., Palla, P. L., Giordano, S., Colombo, L., Jun 2009. Nonlinear elasticity of monolayer graphene. Phys. Rev. Lett. 102, 235502.

Cao, G., 2014. Atomistic studies of mechanical properties of graphene. Polymers 6 (9), 2404–2432.

Cho, J., Luo, J., Daniel, I., 2007. Mechanical characterization of graphite/epoxy nanocomposites by multi-scale analysis. Composites Science and Technology 67 (1112), 2399 – 2407.

Frank, I. W., Tanenbaum, D. M., van der Zande, A. M., McEuen, P. L., 2007. Mechanical properties of suspended graphene sheets. Journal of Vacuum Science Technology B 25 (6), 2558–2561.

Ji, X.-Y., Cao, Y.-P., Feng, X.-Q., 2010. Micromechanics prediction of the effective elastic moduli of graphene sheet-reinforced polymer nanocomposites. Modelling and Simulation in Materials Science and Engineering 18 (4), 045005.

Klusemann, B., Bahm, H., Svendsen, B., 2012. Homogenization methods for multi-phase elastic composites with non-elliptical reinforcements: Comparisons and benchmarks. European Journal of Mechanics - A/Solids 34 (0), 21 – 37.

Lee, C., Wei, X., Kysar, J. W., Hone, J., 2008. Measurement of the elastic properties and intrinsic strength of monolayer graphene. Science 321 (5887), 385–388.

Lee, J.-U., Yoon, D., Cheong, H., 2012. Estimation of youngs modulus of graphene by raman spectroscopy. Nano Letters 12 (9), 4444–4448, pMID: 22866776.

Lu, Q., Gao, W., Huang, R., 2011. Atomistic simulation and continuum modeling of graphene nanoribbons under uniaxial tension. Modelling and Simulation in Materials Science and Engineering 19 (5), 054006.

Lu, Q., Huang, R., 2009. Nonlinear mechanics of single-atomic-layer graphene sheets. International Journal of Applied Mechanics 01 (03), 443–467.

Mori, T., Tanaka, K., 1973. Average stress in matrix and average elastic energy of materials with misfitting inclusions. Acta Metallurgica 21 (5), 571 – 574.

Mura, T., 1991. Micromechanics of Defects in Solids. Kluwer Academic Publishers.

Nozaki, H., Taya, M., Sep. 1997. Elastic fields in a polygon-shaped inclusion with uniform eigenstrains. Journal of Applied Mechanics 64 (3), 495–502.

Nozaki, H., Taya, M., Apr. 2000. Elastic fields in a polyhedral inclusion with uniform eigenstrains and related problems. Journal of Applied Mechanics 68 (3), 441–452.

Rodin, G. J., 1996. Eshelby's inclusion problem for polygons and polyhedra. Journal of the Mechanics and Physics of Solids 44 (12), 1977 – 1995.

Sakhaee-Pour, A., 2009. Elastic properties of single-layered graphene sheet. Solid State Communications 149, 91 – 95.

Sakhaee-Pour, A., Ahmadian, M. T., Naghdabadi, R., 2008. Vibrational analysis of single-layered graphene sheets. Nanotechnology 19 (8), 085702.

Wang, L., Zhang, Q., 2012. Elastic behavior of bilayer graphene under in-plane loadings. Current Applied Physics 12 (4), 1173 – 1177.

Wang, Q., 2010. Simulations of the bending rigidity of graphene. Physics Letters A 374 (9), 1180 – 1183.

Wei, X., Fragneaud, B., Marianetti, C. A., Kysar, J. W., Nov 2009. Nonlinear elastic behavior of graphene: Ab initio calculations to continuum description. Phys. Rev. B 80, 205407.

Xiao, J., Gama, B., Jr., J. G., 2005. An analytical molecular structural mechanics model for the mechanical properties of carbon nanotubes. International Journal of Solids and Structures 42, 3075 – 3092.

Zhang, Y., Pan, C., 2012. Measurements of mechanical properties and number of layers of graphene from nano-indentation. Diamond and Related Materials 24 (0), 1 – 5.

Zhang, Y. Y., Pei, Q. X., Wang, C. M., 2012. Mechanical properties of graphynes under tension: A molecular dynamics study. Applied Physics Letters 101 (8).

Zhao, H., Min, K., Aluru, N. R., 2009. Size and chirality dependent elastic properties of graphene nanoribbons under uniaxial tension. Nano Letters 9 (8), 3012–3015, pMID: 19719113.

Zheng, Q.-S., Zhao, Z.-H., Du, D.-X., 2006. Irreducible structure, symmetry and average of eshelby's tensor fields in isotropic elasticity. Journal of the Mechanics and Physics of Solids 54 (2), 368 – 383.

Zhou, L., Wang, Y., Cao, G., 2013a. Estimating the elastic properties of few-layer graphene from the free-standing indentation response. Journal of Physics Condensed Matter 25(47), 475301.

Zhou, L., Wang, Y., Cao, G., 2013b. van der waals effect on the nanoindentation response of free standing monolayer graphene. Carbon 57 (0), 357 – 362.

Zou, W., He, Q., Huang, M., Zheng, Q., 2010. Eshelby's problem of non-elliptical inclusions. Journal of the Mechanics and Physics of Solids 58 (3), 346 – 372.

Research Highlights

- The linear and non-linear elastic moduli of the Graphene sheet are computed based on the modified Morse potential;
- The Eshelby's tensor is obtained for a rectangular aspect ratio;
- The non-linear stiffness tensor of the Graphene sheet-reinforced polymer composite is derived using the Mori-Tanaka micro-mechanics scheme;
- The anisotropic degree is analysed for different aspect ratio and mass fractions.